Chemical Geology 529 (2019) 119294

Contents lists available at ScienceDirect

Chemical Geology

journal homepage: www.elsevier.com/locate/chemgeo

The impact of ionic strength on the proton reactivity of clay minerals

Weiduo Hao[a,*], Shannon L. Flynn[a,c], Teruhiko Kashiwabara[a,b], Md Samrat Alam[a], Sasiri Bandara[a], Logan Swaren[a], Leslie J. Robbins[a], Daniel S. Alessi[a], Kurt O. Konhauser[a]

[a] Department of Earth & Atmospheric Sciences, University of Alberta, Edmonton, Alberta T6G 2E3, Canada
[b] Center for Submarine Resources, Japan Agency for Marine–Earth Science and Technology (JAMSTEC), 2-15, Natsushimacho, Yokosuka, Kanagawa 2370061, Japan
[c] School of Natural and Environmental Sciences, Newcastle University, Newcastle upon Tyne NE1 7RU, United Kingdom

ARTICLE INFO

Editor: Balz Kamber

Keywords:
Clay minerals
Surface complexation modeling
Trace elementals
Ionic strength

ABSTRACT

The reactivity of clay mineral surfaces exerts a fundamental control on elemental cycling in environmental systems. However, the effect of solution ionic strength (IS) on their reactivity is poorly understood. Here we quantified the effect of changes in IS on clay mineral reactivity through the application of surface complexation modeling (SCM) based on acid-base titration data for three different clay minerals (kaolinite, illite, and montmorillonite). The results demonstrate that the acidity constants (K_a values) for proton interactions on the clay surface vary linearly as a logarithmic function of solution IS, and that proton binding ability is inversely related to solution IS. Two possible explanations for the observed relationship are proposed: (1) solution electrolytes (e.g., Na^+) competitively bind to clay surface sites relative to protons, and (2) that the surface electrostatic field is attenuated by solution electrolytes. We conclude that the impact of increasing solution IS on clay surface reactivity is the result of a weakening negative surface electric field that impacts the surface potential. This mechanism ultimately leads to different adsorption behavior for cations and anions under changing IS conditions. The empirical relationship between K values and IS provided here can be applied to predict clay surface reactivity under varied environmental IS conditions and has specific implications for trace metal behavior in environments, such as estuaries, where changes in IS can be significant.

1. Introduction

As ubiquitous components at Earth's surface, clay minerals play a crucial role in the adsorption of protons and trace metals from solution. Potentiometric titrations coupled with surface complexation modeling (SCM) have increasingly been used to determine clay surface reactivity and quantify proton and metal adsorption onto clay mineral surfaces (Sverjensky and Sahai, 1996; Schroth and Sposito, 1998; Arda et al., 2006; Hizal and Apak, 2006; Tertre et al., 2006; Gu and Evans, 2007, 2008; Liu et al., 2018; Hao et al., 2018). In short, these studies have demonstrated that clay minerals have high surface reactivities and a strong affinity for trace metal adsorption.

However, considerably less work has been directed at determining how variations in solution ionic strength (IS) affect clay surface reactivity and, in turn, impact trace metal adsorption. One such study, by Sinitsyn et al. (2000), investigated the acid-base properties of illite and the sorption of Nd and Eu at 0.01, 0.1, and 1 M ionic strength and demonstrated that the amount of Nd adsorbed was inversely related to IS. Bradbury and Baeyens (2002, 2009) subsequently applied a 2-site, non-electrostatic surface complexation and cation exchange model to describe the protonation, as well as Ni, Co, Eu, and Sn sorption edges, of Na-montmorillonite and illite over a wide range of pH and ionic strength conditions. Alternatively, Gu and Evans, 2008, Gu et al., 2010) applied a constant capacitance surface complexation model (CCM) to potentiometric titration and trace metal (Cd, Cu, Ni, Pb, and Zn) adsorption data for kaolinite and montmorillonite, and similarly demonstrated that the amount of trace metal adsorbed decreases with increasing IS. Other studies have also shown that clay surface reactivity varies as a function of solution IS (Xu et al., 2008; El-Bayaa et al., 2009; Wu et al., 2011). The collective results of these earlier studies on the effects of solution IS on clay reactivity suggest that IS dependent changes can be explained in one of two ways: (1) the competitive adsorption of solution electrolytes (e.g., Na^+, Cl^-) with trace elements for adsorption to clay surface sites (McBride, 1989; Sahai and Sverjensky, 1997; Coppin et al., 2002; Bradl, 2004), or (2) the weakening of the clay mineral's surface electrostatic field, which, in turn, leads to a reduction in the capacity for trace metal adsorption (Kraepiel et al., 1998; Bohn et al., 2002). Distinguishing which of these two mechanisms is

* Corresponding author at: 3-11 Earth Sciences Building, University of Alberta, Edmonton, AB T6G 2E3, Canada.
E-mail address: whao@ualberta.ca (W. Hao).

https://doi.org/10.1016/j.chemgeo.2019.119294
Received 17 June 2019; Received in revised form 4 August 2019; Accepted 4 September 2019
Available online 05 September 2019
0009-2541/

responsible for observed changes in clay mineral surface reactivity as a function of IS is, therefore, essential to understanding how trace metals interact with clay surfaces in environments where stark contrasts in environmental conditions may occur, such as the transition from riverine to estuarine systems.

In theory, the successful prediction of how IS impacts clay surface reactivity and metal adsorption can be evaluated using electrostatic surface complexation models. For example, the diffuse layer model (DLM) and triple layer model (TLM) both incorporate IS as an adjustable parameter for derivation of chemical equilibrium constants (K values) and site concentrations. Although the objective of those models is to derive "intrinsic" chemical equilibrium constants that are independent of solution IS, previous work has highlighted the difficulty in generating IS independent chemical equilibrium constants even when electrostatic models are used (Goldberg, 2005; Landry et al., 2009; Schaller et al., 2009; Reich et al., 2010). A non-electrostatic SCM approach cannot quantify the impact of IS, but it can generate apparent chemical equilibrium constants for metals and/or proton binding at the IS condition being considered. The shortcoming of IS-dependent K values could be alleviated by either developing more mechanistic electrostatic models that properly parameterize the impact of IS or by establishing empirical relationships between IS and chemical equilibrium constants for incorporation into non-electrostatic models.

In this study, three common clay minerals (kaolinite, illite, and montmorillonite) were selected for potentiometric titration to evaluate the impact of IS on their surface reactivity. A non-electrostatic SCM approach was applied to potentiometric titration data to develop a basic framework that considers chemical equilibrium constants and solution IS. The SCM was complimented by metal adsorption experiments to distinguish whether solution electrolyte competition or an attenuation of the electric field strength accounts for the observed changes in clay surface reactivity resulting as a function of changes in solution IS. Unlike purely theoretical and structural models of clay chemistry, the purpose of this paper is to derive applicable knowledge on natural clay materials, and describe how clay surface properties change as a function of fluctuations in the aqueous environment, specifically in regard to changes in IS.

2. Background theory

Surface complexation models based on potentiometric titrations are practical for determining discrete proton exchanging surface ligands. Various models, including both non-electrostatic models (NEM) and electrostatic models (EM), offer a range of mathematical approaches and assumptions regarding electrostatic phenomena. Such models are, however, unified by the ultimate parameterization of chemical equilibrium constants (K values) for proton surface interactions and the concentrations of surface functional groups (site concentrations) (Lalonde et al., 2007; Alessi and Fein, 2010). In general, the adsorption process as described by SCM can be broken down into a system of equations:

$$\equiv XO^- + M^{n+} \leftrightarrow \equiv XO - (M)^{(n-1)+} \quad (R1)$$

$$K = \frac{[\equiv XO - (M)^{(n-1)+}]}{[\equiv XO^-] \bullet \alpha_{M^{n+}}} \quad (1)$$

where $\equiv XO^-$ is the negatively charged surface functional group, M^{n+} is the metal cation or proton of interest, and K is the chemical equilibrium constant for the adsorption reaction. In this notation, the square brackets represent molar concentration and $\alpha_{M}{}^{n+}$ indicates the activity of an aqueous cation. The mass action equation of the NEM is represented by Eq. 1, where the impact of the surface electric field and the IS of solution are not explicitly described. The derived K values from NEM are, therefore, "apparent" and may be represented by K_{app}. Conversely, an EM aims to generate "intrinsic" chemical equilibrium constants (K_{int}) that are independent of aqueous conditions during adsorption (e.g., IS and pH) by separating the electrostatic effect from K_{app} (Hao et al., 2018). In doing so, the Gibbs free energy of ion adsorption onto mineral surfaces is divided into two components: (i) the Gibbs free energy for the reaction of ions binding onto surface functional groups, and (ii) the Gibbs free energy for the work done to move ions from their initial position to the mineral surface(s) by the surface electrostatic field (Sverjensky and Sahai, 1996). With regard to K values, the relationship between EM and NEM, may be represented by the Gouy-Chapman model, where:

$$K_{app} = K_{int} * 10^{\frac{-\Delta Z * F * \Psi}{2.303 * R * T}} \quad (2)$$

where F is the Faraday constant, R is the ideal gas constant, T is temperature in Kelvin, and ΔZ is the change in surface charge. A detailed derivation of this equation is presented in Severjensky and Sahai (1996).

There are three kinds of EMs, each of which is based on different assumptions regarding the relationship between surface charge (δ) and the potential of the surface electric field (Ψ) (Davis and Kent, 1990). The constant capacitance model (CCM), based on Helmholz theory, assumes a constant electrostatic capacitance at clay surfaces, and that the electrostatic potential decreases linearly with increasing distance away from surface. The DLM is designed according to the Gouy-Chapman theory and assumes that there is an accumulation of diffused ions at the surface and that the surface potential decreases exponentially with increasing distance from surface. Finally, the TLM is a combination of the CCM and DLM models. In the TLM, the electrostatic field is divided into three separate layers: two Helmholz layers, and one Gouy-Chapman layer that extends from the solid surface outwards to infinity (Hohl and Stumm, 1976; Davis et al., 1978; Dzombak and Morel, 1990; Kallay et al., 2006). Each of these three EMs is elaborated on in Section 5.4.

3. Methods

Automated titrations of kaolinite (KGa-2), illite (IMt-2), and montmorillonite (SWy-2) were performed at seven IS conditions, spanning two orders of magnitude, using a potentiometric titrator (Metrohm Titrando 905) at the University of Alberta. Sodium nitrate solutions (ACS certified, Fisher Scientific) of 0.001 M, 0.005 M, 0.01 M, 0.025 M, 0.05 M, 0.075 M, and 0.1 M were prepared and used as the background electrolyte in titrations, and each titration was performed in triplicate. Acids and bases (0.1 M HCl and 0.1 M NaOH) were used to adjust pH during each titration. Each of the three clay minerals used in titrations were sodium saturated, and therefore contain little surface-bound or interlayer calcium. The source and pretreatment of clay minerals, and specific experimental conditions are detailed in Hao et al. (2018), and the physical and chemical properties of each of the three clay minerals are provided in the Supplementary Information, Table SI 1. Briefly, all clay minerals were washed in 0.1 M $NaNO_3$ solution for 3 h and freeze-dried before experiments. All titrations were conducted in sealed reaction vessels in which the electrolyte solutions were bubbled with $N_{2(g)}$ for 30 min prior to the initiation of titrations, to avoid contamination with atmospheric $CO_{2(g)}$. Size-fractionation experiments were also performed on three clay minerals to make comparison with raw clay samples, and the experimental methods and results are provided in the Supplementary Information (Table SI 6).

Surface complexation modeling was performed using the resultant data from 63 titration curves spanning the seven IS conditions. Surface functional groups for the clays were assigned to one of two types: ≡LH or ≡XOH, which represent a permanently charged (i.e. structural) surface functional group (one that can only deprotonate) and an amphoteric surface functional group (representing Si—O and Al-OH groups), respectively (Barbier et al., 2000; Peacock and Sherman, 2005; Gu et al., 2010). The protonation behaviors of the permanently charged and amphoteric sites are described as follows:

Table 1
Results of surface complexation modeling summary for kaolinite.

IS	0.001	0.005	0.01	0.025	0.05	0.075	0.1
Log(IS)	-3	−2.301	−2	−1.602	−1.301	−1.125	−1
$LogK_a$	−10.584	−9.785	−10.026	−9.622	−9.299	−9.495	−9.625
STD	0.168	0.699	0.133	0.447	0.556	0.263	0.227
$LogK_{a-}$	−7.765	−7.176	−7.274	−6.785	−6.515	−6.552	−6.539
STD	0.030	0.462	0.266	0.334	0.199	0.242	0.132
$LogK_{a+}$	5.682	5.385	5.346	5.179	4.933	4.877	4.707
STD	0.036	0.139	0.048	0.067	0.197	0.118	0.020

Note: STD means standard deviation, IS means ionic strength.

$$\equiv LH \leftrightarrow H^+ + \equiv L^- \quad (R2)$$

$$K_a = \frac{[\equiv L^-]\bullet\alpha_{H^+}}{[\equiv LH]} \quad (3)$$

$$\equiv XOH \leftrightarrow H^+ + \equiv XO^- \quad (R3)$$

$$K_{a-} = \frac{[\equiv XO^-]\bullet\alpha_{H^+}}{[\equiv XOH]} \quad (4)$$

$$\equiv XOH + H^+ \leftrightarrow \equiv XOH_2^+ \quad (R4)$$

$$K_{a+} = \frac{[\equiv XOH_2^+]}{[\equiv XOH]\bullet\alpha_{H^+}} \quad (5)$$

where, square brackets denote the concentration of surface functional groups and α_{H+} the activity of protons in solution; K values derived by Eqs. 3, 4 and 5 are proton interaction constants that govern the adsorption and desorption of protons from the clay surface. To examine the impact of changing IS on the surface electrostatic field, a NEM at each of the seven IS conditions was generated using the titration data and the modeling software FITEQL 4.0 (Westall, 1982) in order to calculate K_{app} for each of the three clay minerals at the given IS.

The range of IS conditions investigated spans two orders of magnitude, and the activity of aqueous species was accounted for in the SCM using the Debye-Huckel equation (Eq. 6) through which activity coefficients (γ) were calculated. The corresponding activity for H^+ (α_{H+}) (Eq. 7) was then used in the SCM (Langmuir, 1997).

$$\log\ \gamma = -Az_i^2\sqrt{I}\,(1 + Ba_i\sqrt{I}) \quad (6)$$

$$\alpha_{H+} = \gamma * [H^+] \quad (7)$$

where A and B are empirical constants that are a function of the density, dielectric constant, and temperature of water, z_i is the charge of the ion, a_i is a size parameter, I is the ionic strength, and $[H^+]$ is the molar concentration of protons (see Ref. Langmuir (1997) for a detailed description).

Anion adsorption experiments can be applied to test whether the impact of ionic strength on clay surface reactivity is due to a weakening surface electrostatic field or competitive adsorption. Here, we performed chromate, Cr(VI), adsorption experiments at 0.001 M and 0.1 M $NaNO_3$ for each of the three clay minerals to examine the impact of IS on Cr(VI) adsorption. A 0.001 M stock solution was made by first adding 0.017 g of $NaNO_3$ (ACS grade) to a 200 mL volumetric flask, and then 2 mL of a 2 mM Cr(VI) stock solution was added, followed by dilution with DI water to a final volume of 200 mL. The resulting solution contained 0.001 M $NaNO_3$ and 1 mg/kg Cr(VI). The 0.1 M IS solution was made in a similar manner, but 1.7 g of $NaNO_3$ was added. For adsorption experiments, 25 mL of each the above solution was mixed with 0.25 g of each clay to achieve a clay concentration of 10 g/L. The adsorption experiments were then allowed to equilibrate for 48 h and the pH of each tube was adjusted to pH 5 because a considerable amount of negatively-charged chromate (CrO_4^{2-}) would be adsorbed to the clays due to a lesser overall net-negative charge of the clays versus at higher pH values (Liu et al., 2018; Veselska et al., 2016). The pH was continuously adjusted through the addition of small aliquots of either 0.1 M HNO_3 and NaOH (ACS grade) until a stable pH was achieved. Once equilibrium was reached, 5 mL of each solution was taken by pipet and filtered through a 0.2 μm membrane for measurement on an Agilent 8800 ICP-MS/MS at the Environmental Geochemistry Lab at the University of Alberta. All samples for ICP-MS analysis were diluted 50 times to avoid matrix effects. An internal standard of 1 mg/kg Indium was added to all samples and used to monitor instrumental drift during analysis. The standard deviation of ICP-MS measurement was < 3%, as calculated by the triplicate analysis of each sample.

4. Results

4.1. Surface complexation modeling

Our modeling results are in excellent agreement with experimental results, validating of our modeling procedure (Supplementary Information 2, Figs. SI 1–4). K values for the surface reactions calculated through the SCM approach are listed in Tables 1, 2, and 3 for kaolinite, illite, and montmorillonite, respectively (details of the triplicates are provided in Supplementary Information 3, Tables SI 2–4). For kaolinite, the $logK_a$, $logK_{a-}$ and $logK_{a+}$ values vary from −9.6 to −10.6, −6.5 to −7.8, and 4.7 to 5.7, respectively, as IS increases. Compared to kaolinite, illite has higher $logK_a$ and $logK_{a+}$ values which range from −6.3 to −5.5, and 9.8 to 9.5, respectively, but a lower K_{a-} (−11.4 to −10.4) (Table 2). The $logK_a$ and $logK_{a-}$ of montmorillonite are similar to those of illite, but the $logK_{a+}$ of montmorillonite is higher and ranges from 9.8 to 10.1. (Table 3). For all three clay minerals, the

Table 2
Results of surface complexation modeling summary for illite.

IS	0.001	0.005	0.01	0.025	0.05	0.075	0.1
Log(IS)	−3	−2.301	−2	−1.602	−1.301	−1.125	−1
$LogK_a$	−6.288	−5.995	−5.917	−5.793	−5.670	−5.556	−5.488
STD	0.017	0.053	0.055	0.029	0.045	0.062	0.148
$LogK_{a-}$	−11.419	−11.118	−10.119	−11.166	−10.611	−10.671	−10.408
STD	0.401	0.452	0.038	0.130	0.312	0.146	0.388
$LogK_{a+}$	9.825	9.715	9.734	9.629	9.554	9.473	9.579
STD	0.034	0.075	0.008	0.022	0.077	0.033	0.103

Table 3
Results of surface complexation modeling summary for montmorillonite.

IS	0.001	0.005	0.01	0.025	0.05	0.075	0.1
Log(IS)	−3	−2.301	−2	−1.602	−1.301	−1.125	−1
$LogK_a$	−5.997	−5.759	−5.661	−5.560	−5.567	−5.478	−5.699
STD	0.062	0.051	0.041	0.061	0.062	0.054	0.131
$LogK_{a-}$	−11.126	−10.990	−10.850	−10.884	−10.818	−10.715	−10.566
STD	0.643	0.341	0.488	0.146	0.143	0.283	0.149
$LogK_{a+}$	10.133	10.060	9.988	9.875	9.871	9.858	9.833
STD	0.094	0.036	0.050	0.041	0.141	0.017	0.153

standard deviation is generally small compared to the K values. Illite and montmorillonite's proton reaction constants are very similar. In contrast, kaolinite's proton reaction constants differ from those of illite and montmorillonite's $logK_a$, $logK_{a-}$ and $logK_{a+}$.

Previous studies have applied the cation exchange reaction ($\equiv LH + Na^+ \leftrightarrow H^+ + \equiv LNa$) for $\equiv LH$ sites (e.g. Gu and Evans, 2007, 2008). In this manuscript, the primary purpose is to investigate the impact of solution electrolyte on clay surface reactivity, that is, whether competitive adsorption or a weakening surface electrostatic field best explains sorption behavior. In previous studies the approach taken has led to competitive adsorption being assumed in the first place, without knowing if it is actually the case. Nonetheless, for the sake of comparison with previous data and to demonstrate our linear trend is robust, we provide modeling results applying cation exchange reaction as described above in the Supplementary Information.

4.2. Proton interaction constants as a function of ionic strength

Our modeling results show an increase in $logK_a$ and $logK_{a-}$ but a decrease in $logK_{a+}$ with increasing IS for all three clay minerals. Figs. 1, 2, and 3 show the empirical relationship between solution IS and the proton interaction constants for each of the three clay minerals. When plotted as a function of log(IS), a linear relationship with the $logK_{app}$ becomes apparent. The linear equations were fitted in Origin 9.1 and are defined as:

$$logK_{app} = m * log(IS) + b \quad (8)$$

The specific values for m and b for each of the three clay minerals are provided in Table 4. The intercept of this equation (b) represents the presumed logK value of the clay at highly saline conditions (1 M) where log(IS) = 0, while the slope (m) quantifies how the clay surface reactivity varies with ionic strength. Most of the proton interaction values are highly correlated with solution IS (Table 4), with the exception of the $logK_{a-}$ of illite ($R^2 = 0.3516$), which may be the result of an anomalous point in the 0.01 M titration. Additionally, montmorillonite has a higher variability between triplicates than kaolinite or illite; this may be attributed to the swelling nature of montmorillonite.

4.3. Chromium adsorption onto three clay minerals

The results of Cr(VI) adsorption experiments are listed in Table 5. The amount of Cr adsorbed onto three clay minerals was generally low (< 1 mg/kg), likely the result of Cr(VI) being present as an oxyanion (CrO_4^{2-}) and, therefore, subject to a repulsive force at the negatively charged clay surfaces. At the low IS condition (0.001 M), kaolinite can adsorb more Cr(VI) compared to the high IS condition (0.1 M), while for montmorillonite and illite, the amount of Cr(VI) adsorbed at 0.1 M is higher than that at 0.001 M.

5. Discussion

5.1. The comparison of surface proton reactivity among clay minerals

Illite and montmorillonite have $logK_{a+}$, $logK_{a-}$ values between 9.5 and 9.8 and −10.4 to −11.4, respectively. This means that the illite and montmorillonite ≡XOH groups are largely protonated at neutral pH conditions, while the range of $logK_a$ values from −6.3 to −5.5 indicates that the ≡LH groups may become either deprotonated or

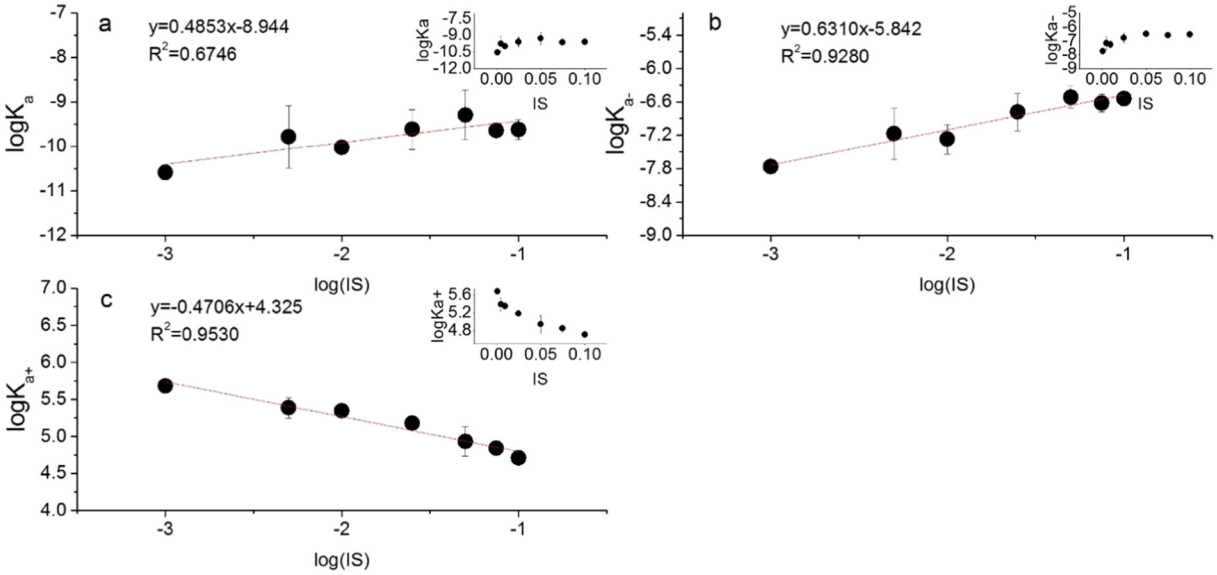

Fig. 1. Proton interaction constants of kaolinite and their relationship with ionic strength. (a) $logK_a$ change with solution IS; (b) $logK_{a-}$ variation with solution IS; and (c) the relationship between $logK_{a+}$ and solution IS.

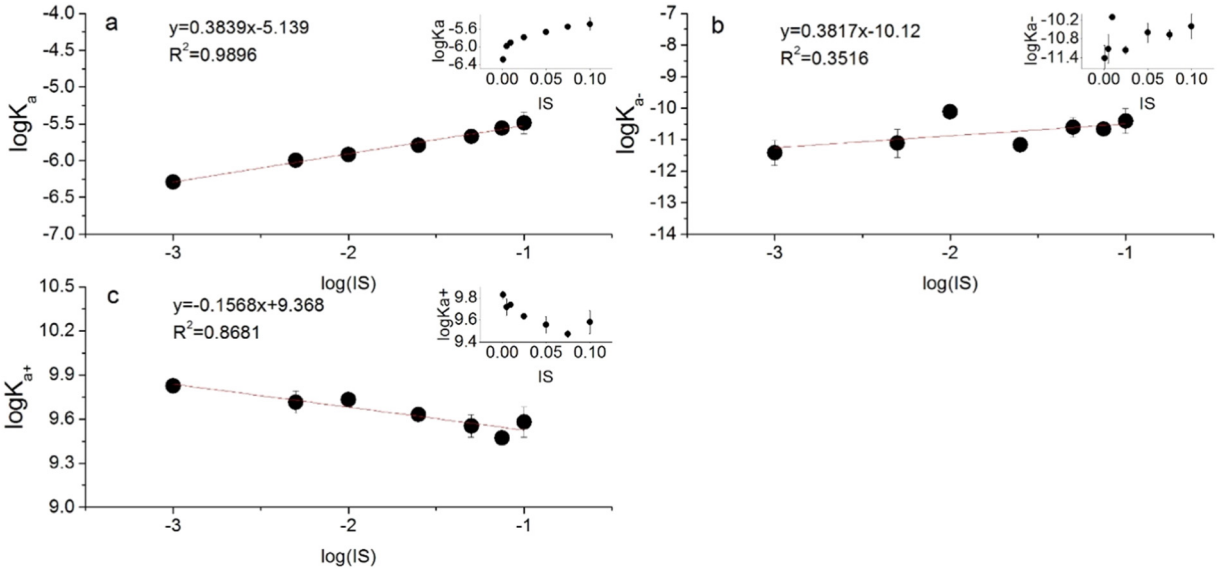

Fig. 2. Proton interaction constants of illite and their relationship with ionic strength. (a) $logK_a$ change with solution IS; (b) $logK_{a-}$ variation with solution IS; and (c) the relationship between $logK_{a+}$ and solution IS.

protonated at a pH near 6, as pH is increased or decreased, respectively. In contrast, kaolinite's $logK_a$ values indicate that the ≡LH site is protonated until around pH 10, while the ≡XOH site can be protonated and deprotonated between pH 5 and 6.

The titration results for size-fractionation clay shows that the < 2 μm clay fraction has lower $logK_a$ values for montmorillonite and illite, but $logK_{a-}$ and $logK_{a+}$ values are nearly identical to those of the raw clay. Size fractionated kaolinite cannot be modeled with the current modeling method, which can only be modeled through either one amphoteric site model or two sites deprotonation model. The decreasing in $logK_a$ indicates that the < 2 μm clay fraction has stronger proton binding on the ≡LH site than does the bulk clay.

Previously published proton interaction constants for clay minerals vary significantly. For example, the $logK_a$ value for the ≡XOH site of montmorillonite is −10.5 according to Baeyens and Bradbury (1997), while Barbier et al. (2000) derived a value of −5.26 for the same site. A detailed compilation of literature K values for clay adsorption sites is

Table 4
Mathematical relationship between K values and ionic strength (IS).

		m	b	R^2
Kaolinite	$logK_a$	0.485	−8.944	0.675
	$logK_{a-}$	0.631	−5.842	0.928
	$logK_{a+}$	−0.471	4.325	0.953
Illite	$logK_a$	0.384	−5.139	0.990
	$logK_{a-}$	0.382	−10.120	0.352
	$logK_{a+}$	−0.157	9.368	0.868
Montmorillonite	$logK_a$	0.199	−5.324	0.698
	$logK_{a-}$	0.235	−10.440	0.869
	$logK_{a+}$	−0.158	9.667	0.960

Note: m and b are slope and intercept, respectively, of the linear relationship between proton interaction constants and IS (in Eq. 7), and R^2 is the correlation coefficient of the linear relationship.

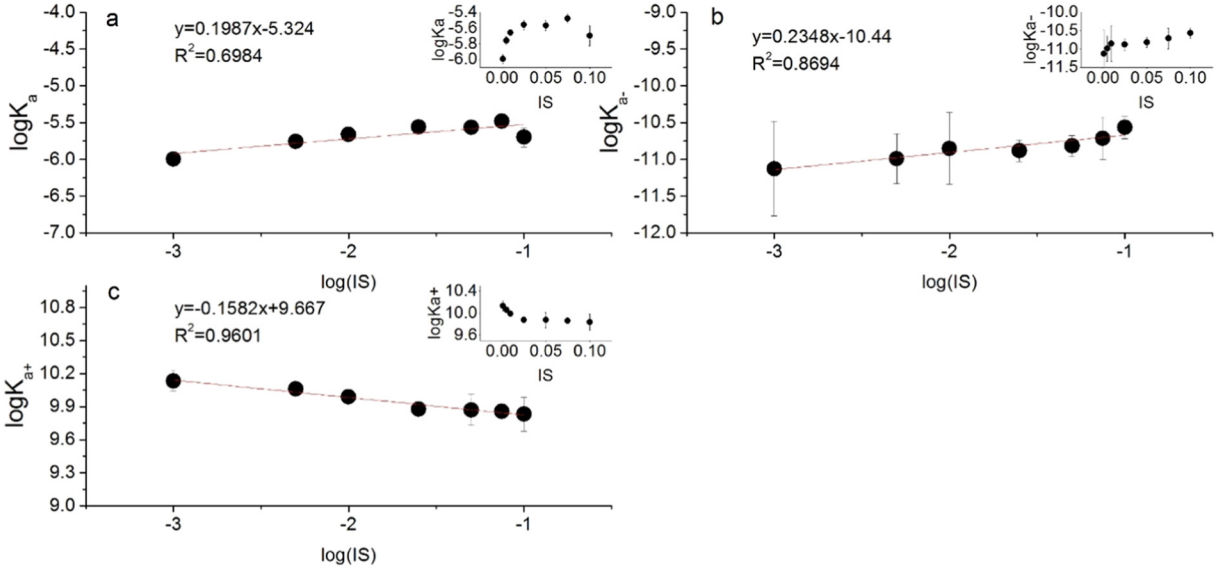

Fig. 3. Proton interaction constants of montmorillonite and their relationship with ionic strength. (a) $logK_a$ change with solution IS; (b) $logK_{a-}$ variation with solution IS; and (c) the relationship between $logK_{a+}$ and solution IS.

Table 5
Degree of chromium adsorption onto three clay minerals at two IS conditions.

		Adsorbed (mg/kg)	STD
Kaolinite	IS = 0.001 M	0.403	0.016
	IS = 0.1 M	0.247	0.018
Montmorillonite	IS = 0.001 M	0.190	0.011
	IS = 0.1 M	0.206	0.015
Illite	IS = 0.001 M	0.084	0.005
	IS = 0.1 M	0.152	0.012

provided by Gu and Evans (2007, 2008) and Gu et al. (2010). Differences in values reported in the literature may be attributed to heterogeneity in natural samples that result in differing values between batches, additionally, varied modeling assumptions and experimental conditions likely also contribute to these differences. For example, some literature K values for the permanently charged site have modeled it as an ion exchange site ($\equiv LNa \leftrightarrow Na^+ + \equiv L^-$) (Lackovic et al., 2003; Ikhsan et al., 2005), which leads to K values that differ than those derived here. Moreover, EMs will have lower absolute logK values compared to NEMs, as EMs separate the electrostatic effect from the constant, while the logK derived from NEMs represents a combination of the chemical affinity and electrostatic effect. This may explain why our data has higher absolute values compared to the existing literature values. Other factors influencing the calculation of K values may include contamination by atmospheric $CO_{2(g)}$ during the titration process (see Hao et al. (2018)) as well as the method of clay pretreatment. In the latter case, work by Liu et al. (2018), using the same three clay minerals, resulted in lower absolute K values, but in this case the clays were pretreated with acid. The acid treatment increases the surface area of the clay particles by partially solubilizing Al and Si. The structural charge of the acidic treated clay increases due to the loss of octahedral and tetrahedral elements like Al and Si (Hao et al., 2019).

5.2. The competitive adsorption of solution electrolytes

With increasing IS, both the K_a and K_{a-} values for each of the three studied clay minerals increase, while the K_{a+} value decreases (Figs. 1-3). This pattern indicates a clear decrease in the proton binding ability at higher IS, as the requisite pH for ≡LH deprotonation and ≡XOH site deprotonation/protonation decreases with increasing IS. One possibility is that the change in K_{app} that accompanies increasing IS can be explained by the competitive adsorption of solution electrolytes onto the clay surface. To test this possibility, the Na^+ adsorption constant (K_{Na}) can be modeled. By incorporating K_{Na} into our SCM models at various IS titration data, IS-independent chemical equilibrium constants should be derived if the competitive adsorption of solution electrolytes is responsible for the observed trend.

To model K_{Na}, the clay minerals were titrated in ultrapure water with the same method used in the titration experiments and the same SCM approach for the calculation of K values was applied. This ultrapure titration data was then considered to represent the same system of equations without a Na^+ binding reaction being included (the pre-existing Na^+ concentration on the surface was analyzed; detailed information can be seen in Supplementary Information, Fig. SI 5). An iterative approach (see Alessi et al. (2010)) was applied to the titration data from the seven IS experiments for three clay minerals to calculate K_{Na}:

$$\equiv LH + Na^+ \leftrightarrow \equiv LNa + H^+ \quad (R5)$$

$$K_{LNa} = \frac{[\equiv LNa]\cdot\alpha_{H^+}}{[\equiv LH]\cdot\alpha_{Na^+}} \quad (9)$$

$$\equiv XOH + Na^+ \leftrightarrow \equiv XONa + H^+ \quad (R6)$$

Table 6
Na^+ binding constants on the two surface functional groups of the three clay minerals.

Log(IS)	IS	$logK_{LNa}$	STD	$logK_{XONa}$	STD
Kaolinite					
−3	0.001	−6.981	0.231	−169	0
−2.301	0.005	−8.410	0.106	−3.237	0.413
−2	0.01	−7.606	0.114	−170	0
−1.602	0.025	−8.125	0.018	−170	0
−1.301	0.05	−8.587	0.263	−59.071	96.934
−1.125	0.075	−8.062	0.110	−115.222	96.610
−1	0.1	−8.266	0.040	−171	0
Illite					
−3	0.001	−3.362	0.360	−169	0
−2.301	0.005	−3.635	0.258	−170	0
−2	0.01	−3.256	0.104	−170	0
−1.602	0.025	−3.398	0.124	−171	0
−1.301	0.05	−3.559	0.060	−171	0
−1.125	0.075	−3.570	0.087	−171	0
−1	0.1	−3.355	0.119	−170.965	0.061
Montmorillonite					
−3	0.001	−3.111	0.424	−8.144	1.244
−2.301	0.005	−3.355	0.955	−8.885	0.003
−2	0.01	−3.201	0.511	−8.709	0.430
−1.602	0.025	−3.263	0.612	−9.234	0.454
−1.301	0.05	−3.322	0.518	−9.388	0.231
−1.125	0.075	−3.032	0.351	−9.529	0.177
−1	0.1	−2.959	0.852	−9.476	0.337

$$K_{XONa} = \frac{[\equiv XONa]\cdot\alpha_{H^+}}{[\equiv XOH]\cdot\alpha_{Na^+}} \quad (10)$$

To be specific, the K values of surface protonation/deprotonation reactions in pure water titration were input into the SCM model for parameterizing $logK_{LNa}$ and $logK_{XONa}$ with the known initial Na^+ concentrations for each titration. The $logK_{Na}$ values for each of the clay minerals are provided in Table 6. For all three clays, the $logK_{XONa}$ values are exceedingly low (approaching −170), indicating that Na^+ binding on the amphoteric site is effectively negligible. The $logK_{LNa}$ for kaolinite is lower than that of illite and montmorillonite, indicating that the Na^+ binding capacity of kaolinite is less than that of illite and montmorillonite. A plot of $logK_{LNa}$ versus IS shows a relatively constant K_{LNa} across the range of IS conditions considered here (Fig. 4).

Most SCM models of titration with K_{Na} incorporated fail to converge (detailed systematic equations are provided in the Supplementary Information), indicating that the adsorption of Na^+ is unlikely to explain the change in K_{app} values for proton interactions observed with increasing IS. To further test the effect of competitive Na^+ adsorption, the corresponding binding constants were incorporated into a NEM for Cd adsorption onto clay minerals at varied IS using literature Cd adsorption data (Gu and Evans, 2007, 2008; Gu et al., 2010). The Cd adsorption model is detailed below, and the results summarized in Supplementary Information, Table SI 5.

$$\equiv LH + Cd^{2+} \leftrightarrow \equiv LCd^+ + H^+ \quad (R7)$$

$$K_{LCd} = \frac{[\equiv LCd^+]\cdot\alpha_{H^+}}{[\equiv LH]\cdot\alpha_{Cd^{2+}}} \quad (11)$$

$$\equiv XOH + Cd^{2+} \leftrightarrow \equiv XOCd^+ + H^+ \quad (R8)$$

$$K_{XOCd} = \frac{[\equiv XOCd^+]\cdot\alpha_{H^+}}{[\equiv XOH]\cdot\alpha_{Cd^{2+}}} \quad (12)$$

After including Na^+ binding, the results still produce IS dependent values for both K_{LCd} and K_{XOCd} (Supplementary Information, Table SI 5), where K_{LCd} shows a decreasing trend with increasing IS for all three clays, and K_{XOCd} increases with IS, except for kaolinite. This is consistent with previous research that has shown trace metals tend to adsorb primarily to permanently charged sites via cation exchange at low

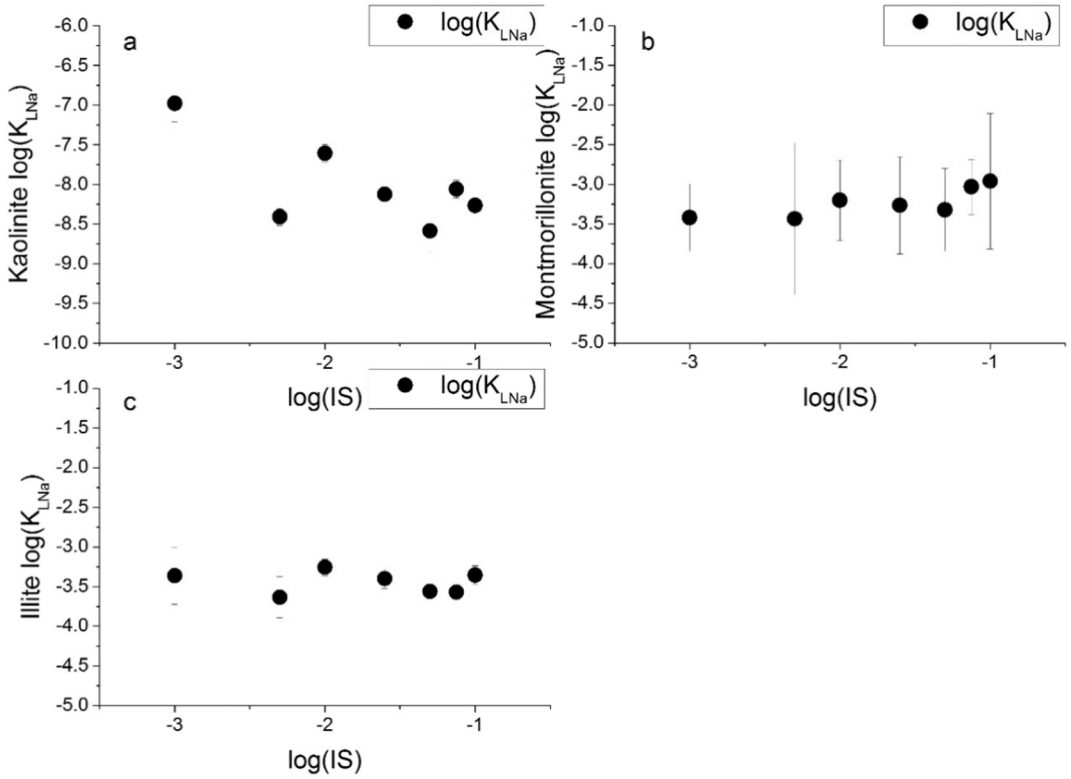

Fig. 4. The change in the Na^+ binding constant ($logK_a$) with changing IS for all three clay minerals: (a) kaolinite; (b) montmorillonite and (c) illite.

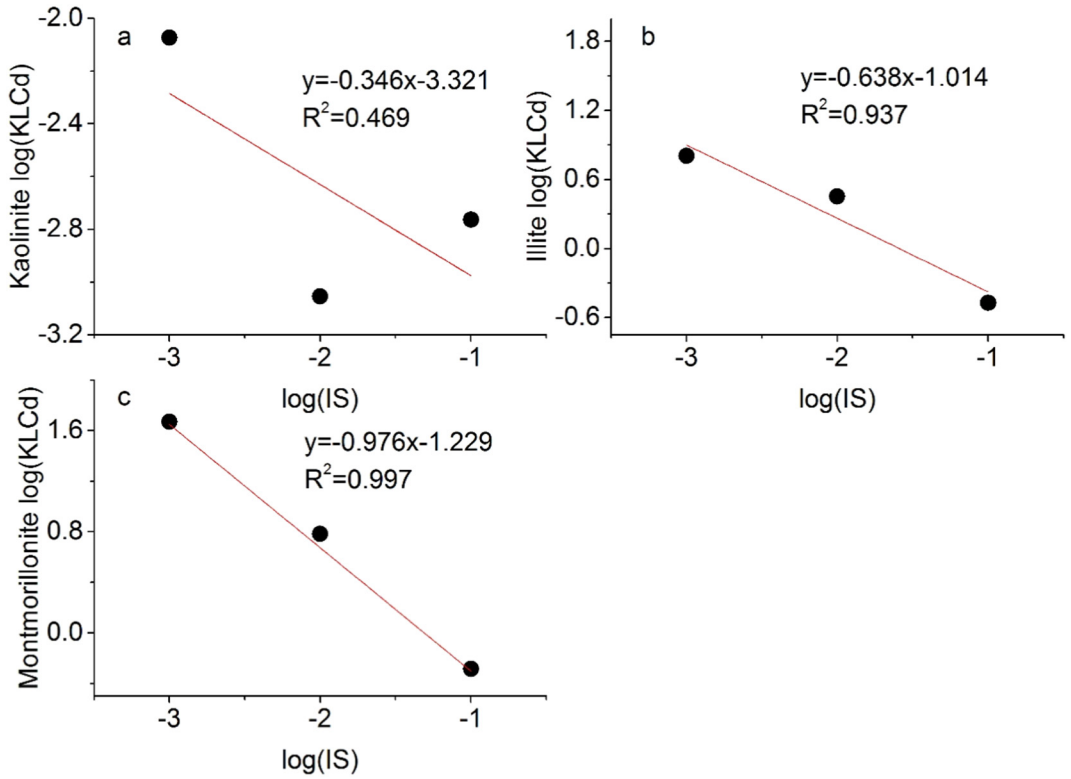

Fig. 5. Change in the Cd binding constant ($logK_{LCd}$) of the permanently charged site ($logK_{LCd}$) with IS for three clay minerals: (a) kaolinite; (b) illite; and (c) montmorillonite.

IS condition, and mainly onto amphoteric sites at high IS condition (Morton et al., 2001). The exception of kaolinite may be attributed to its lower permanent charge (Sposito et al., 1999). The plot of K_{LCd} values versus log(IS) produces a linear relationship which is similar to the relationship observed between log(IS) and $logK_a$, $logK_{a+}$, $logK_{a-}$ (Fig. 5), suggesting that, despite incorporating K_{Na} into our NEM, the SCM approach still fails to capture the inherent variability of K_{app} values as a function of IS.

Our results indicate that the sorption of monovalent electrolyte ions, such as Na^+, cannot account for the IS dependent nature of the K values for clay minerals as calculated by SCM. For inorganic clay surfaces, H^+ preferentially adsorbs, while other ions, such as K^+, Na^+, NO_3^-, and Cl^-, only weakly adsorb to the surface (Davis et al., 1978).

5.3. Attenuation of the surface electrostatic field by increasing ionic strength

The change in K_{app} with solution IS may also be attributed to the attenuation of the surface electrostatic field as IS increases. However, there is no direct method to quantify the surface electric field and only a theoretical estimation can be made. Sverjensky and Sahai (1996) demonstrated that K_{int} values for surface protonation reactions are solely influenced by the surface properties of the solid and the specific surface reaction. Therefore, for a surface reaction, K_{int} is independent of solution IS, while K_{app} shows a direct relationship with IS as indicated by our experimental results (Eq. 8). The relationship between surface electric field and solution IS can be derived by substituting Eq. 8 into Eq. 2:

$$\Psi = \frac{2.303RT}{\Delta ZF} * (\log K_{int} - [m * \log(IS) + b]) \quad (13)$$

where, m and b are the slope and intercept generated from our experimental results, respectively. By simplifying all the constants Eq. 13 can be written as:

$$\Psi = N_1 - N_2[m * \log(IS) + b] \quad (14)$$

where, m, b, are the slope and intercept of Eq. 8; N_1, N_2 are all constants, representing $\frac{2.303RT}{\Delta ZF}\log K_{int}$ and $\frac{2.303RT}{\Delta ZF}$, respectively. As is evident from Eq. 14, surface potential is inversely related to the IS of the solution, indicating the electrostatic field becomes weaker at higher IS.

Negatively-charged clay surfaces promote cation adsorption and tend to limit the degree of anion adsorption. If attenuation of the surface electric field is the mechanism by which solution IS influences the adsorption process, an increase in IS will lead to a decrease in trace metal cation adsorption and a corresponding increase in trace anion adsorption. However, if the competitive adsorption of solution electrolytes is the mechanism, the result would be a decrease of both cation and anion adsorption as IS increases. The decrease in cation adsorption that accompanies an increase in IS has been well documented (Gu and Evans, 2007, 2008; Gu et al., 2010). A direct way to distinguish which of these two mechanisms is operative is to observe the anion adsorption behavior at different IS. To this end, we conducted Cr(VI) adsorption experiments onto the three clay minerals at different IS (Table 5). Results showed that for illite and montmorillonite, which have a higher structural charge (Sposito et al., 1999), the amount of CrO_4^{2-} adsorbed onto clay surfaces at IS = 0.1 M is higher than that at IS = 0.001 M. This is because the increased IS led to a weakening of the negative surface electric field, which subsequently promoted the increased adsorption of CrO_4^{2-}.

Interestingly, the above trend is not observed for kaolinite, probably because kaolinite has a lower structural charge compared to illite and montmorillonite (Sposito et al., 1999). In this regard, previous studies have shown that more B(III) (speciated as the ion borate, $B(OH)_4^-$, at neutral to alkaline pH) can adsorb onto montmorillonite at greater concentrations at high IS (Goldberg, 2005), while As(V), which forms the oxyanion arsenate (AsO_4^{3-}), shows higher affinity to soil samples dominated by clay minerals at higher IS when pH is above 5 (Xu et al., 2009). An exception to this general trend, is U. At pH conditions below 6, the adsorption of U(VI) onto kaolinite and montmorillonite is inhibited by increasing IS, while the adsorption is enhanced at pH conditions above 6 (Bachmaf and Merkel, 2011). This occurs because at around pH 6, U(VI) aqueous species shift from the positive uranyl ion (UO_2^{2+}) to negative charged uranyl carbonate ion ($UO_2(CO_3)_3^{4-}$).

It should be noted that while electrostatic field effects influence the amount of metal/proton adsorption onto clay surfaces, there are other considerations. For instance, detailed molecular information regarding the formation of inner-sphere versus outer-sphere complexes can be accessed through spectroscopic methods and may provide useful information for predicting differences in the adsorptive behavior of trace metals at varied IS (Kashiwabara et al., 2011; Gu et al., 2016; Wang et al., 2018).

5.4. The inability of SCMs to produce an ionic strength independent proton interaction constant for clay minerals

The K_{app} derived from NEMs should have an IS dependent signature because K_{app} does not separate the electrostatic factor, and IS has been shown to be capable of influencing the surface electric field. The CCM incorporates an electrostatic term by assuming the surface electrical capacitance (C) is a constant at the mineral-water interface, where the relationship between plane charge (δ) and surface potential (Ψ) is defined as:

$$\Psi = \frac{\delta}{C} \quad (15)$$

Since the CCM fails to consider the impact that varied IS may have, it is not surprising that the CCM derived K values display an IS dependent character (Gu and Evans, 2007, 2008; Gu et al., 2010). The DLM assumes that the electrolyte ions diffuse around the mineral surface, and that the surface potential is related to the plane charge (δ), solution IS (I), and dielectric constant (ε):

$$\Psi = \frac{2RT}{F} * arsinh\left(-\delta/\sqrt{8RT\varepsilon IS}\right) \quad (16)$$

Finally, the TLM divides the electric field into three layers: the first two are CCM-type layers that have different capacitances, and the third is a diffuse layer. Both the DLM and TLM incorporate IS into the modeling procedure, and thus theoretically the K values derived from both models should display an IS independent character. Yet, previous experimental results and arguments contradict this notion (Goldberg, 2005; Landry et al., 2009; Schaller et al., 2009; Reich et al., 2010), which indicates that K values derived from both electrostatic models are not constant with varying ionic strength. In our titration modeling, CCM can successfully simulate experimental data, but produces IS dependent K values as well. Both DLM and TLM iterations fail to converge, indicating that when IS is included as an input parameter, these electrostatic models fail to provide a satisfactory fit for the observed proton interaction behavior.

The IS dependent results of EMs may be the result of our SCM approaches failing to properly account for the inherent structural charge of clay minerals. The surface charge calculation for titration data in the SCM methodology is based on the net surface protonation and deprotonation reactions. However, for clay minerals, surface charge includes both the charge produced by proton interactions and the inherent permanent charge imparted to the clay by isomorphic substitution. This permanent charge cannot be accounted for through SCM simulations when applying EMs. This is particularly true for three-layer clays, such as illite and montmorillonite, that have a tetrahedral-octahedral-tetrahedral sheet structure (TOT type clays) in which isomorphic substitution on the octahedral and tetrahedral sheets leads to the development of a permanent surface charge within the clay structure. Nonetheless, the shielding effect of solution electrolytes with regards to the surface electrostatic field can be significant, especially when one considers the existence of a strong negative surface field at clay mineral surfaces as indicated by the zeta potential (Chorom and Rengasamy, 1995; Vane and Zang, 1997; Kaya and Yukselen, 2005). This defect in accurately simulating the permanent surface charge of clay minerals may be the reason why electrostatic SCMs are unable to generate IS independent K values for these surfaces. It is worth noting that this shielding effect may be assessed through running NEMs at different IS values. The linear relationship between log(IS) and the $\log K_{app}$ determined by

NEMs thereby provides an alternative empirical way for assessing clay surface reactivity at various IS conditions and offers a simpler approach than the development of complicated electrostatic models.

6. Conclusions

Variations in solution IS lead to changes in the derived K_{app} values for the clay minerals, kaolinite, illite, and montmorillonite. The relationship between K_{app} and IS was found to have a linear correlation when plotted in log-log space, and indicates that there is a decrease in the proton adsorption ability of clay minerals with increasing IS. A detailed discussion of our experimental data reveals that the mechanism underlying the impact of changing IS on adsorptive process at the clay mineral surface is the attenuation of the surface electrostatic field. To this end, an empirical equation relating surface potential and environmental IS was derived that potentially can be used to better model and predict the contribution of clay minerals to trace element sequestration in environments with dynamic, changing IS conditions. Indeed, understanding the influence that IS has on the adsorption of trace metals to clay surfaces is an underexplored aspect of interpreting the geological past, such as the record of trace metal availability through time as recorded by the shale record. Shales have been used to track changes in paleomarine chemistry based on a first-order relationship that exists between trace metal concentrations in shale and in seawater from which they were deposited (Tribovillard et al., 2006; Scott et al., 2008; Lyons et al., 2009; Scott et al., 2013; Partin et al., 2013; Reinhard et al., 2013; Reinhard et al., 2017). Natural environments, however, such as estuaries are subject to strong changes in the IS. It is possible that when low IS rivers transport clay minerals sourced from the continents into the high IS ocean, the increase in environmental IS could lead to the release of cations that were adsorbed onto the surface of clay minerals, while at the same time promoting an increase in the adsorption and removal of anions. There is of course a caveat to this simplifying statement because metal behavior in estuaries is influenced by several factors that may include, but are by no means limited to, competitive adsorption, co-precipitation, and the prevailing redox conditions, the variation of clay surface reactivity may also be a significant factor that requires further evaluation. In this regard, future work is needed to assess the trace metal behavior, for both cations and anions, in an estuarine environment to better understand how changes in environmental IS may affect the interpretation of the shale record.

Acknowledgements

HWD gratefully acknowledges the support of China Scholarship Council award (CSC, No. 201506420044), LJR gratefully acknowledges the support of a Vanier Canada Graduate Scholarship, and KT gratefully acknowledges the support of JSPS Grant-in-Aid for Scientific Research No. JP17H06455. This work was supported by NSERC Canadian Network for Research and Innovation in Machining Technology Discovery Grants to KOK (RGPIN-165831) and DSA (RGPIN-04134). Additionally, an NSERC RTI to KOK and DSA supported the purchase of a Metrohm Titrando 905 titrator used in this work.

Appendix A. Supplementary data

Supplementary data to this article can be found online at https://doi.org/10.1016/j.chemgeo.2019.119294.

References

Alessi, D.S., Fein, J.B., 2010. Cadmium adsorption to mixtures of soil components: testing the component additivity approach. Chem. Geol. 270, 186–195.
Alessi, D.S., Henderson, J.M., Fein, J.B., 2010. Experimental measurement of monovalent cation adsorption onto Bacillus subtilis cells. Geomicrobiol J. 27, 464–472.
Arda, D., Hizal, J., Apak, R., 2006. Surface complexation modelling of uranyl adsorption onto kaolinite based clay minerals using FITEQL 3.2. Radiochim. Acta 94, 835–844.
Bachmaf, S., Merkel, B.J., 2011. Sorption of uranium(VI) at the clay mineral-water interface. Environmental Earth Science 63, 925–934.
Baeyens, B., Bradbury, M.H., 1997. A mechanistic description of Ni and Zn sorption on Na-montmorillonite 1. Titration and sorption measurements. J. Contam. Hydrol. 27, 199–222.
Barbier, F., Duc, G., Petit-Ramel, M., 2000. Adsorption of lead and cadmium ions from aqueous solution to the montmorillonite/water interface. Colloids and Surfaces A 166, 153–159.
Bohn, H.L., Myer, R.A., O'Connor, G.A., 2002. Soil Chemistry. John Wiley & Sons.
Bradbury, M.H., Baeyens, B., 2002. Sorption of Eu on Na- and Ca-montmorillonites: Experimental investigations and modelling with cation exchange and surface complexation. Geochimica Cosmochimica Acta 66, 2325–2334.
Bradbury, M.H., Baeyens, B., 2009. Sorption modelling on illite part I: titration measurements and the sorption of Ni, Co, Eu and Sn. Geochimica Cosmochimica Acta 73, 990–1003.
Bradl, H.B., 2004. Adsorption of heavy metal ions on soils and soils constituents. J. Colloid Interface Sci. 277, 1–18.
Chorom, M., Rengasamy, P., 1995. Dispersion and zeta potential of pure clays as related to net particle charge under varying pH, electrolyte concentration and cation type. Eur. J. Soil Sci. 46, 657–665.
Coppin, F., Berger, G., Bauer, A., Castet, S., Loubet, M., 2002. Sorption of lanthanides on smectite and kaolinite. Chem. Geol. 182, 57–68.
Davis, J.A., Kent, D.B., 1990. Surface complexation modeling in aqueous geochemistry. Reviews Mineralogy and Geochemistry 23, 177–260.
Davis, J.A., James, R.O., Leckie, J.O., 1978. Surface ionization and complexation at the oxide/water interface: I. Computation of electrical double layer properties in simple electrolytes. J. Colloid Interface Sci. 63, 480–499.
Dzombak, D.A., Morel, F.M., 1990. Surface Complexation Modeling: Hydrous Ferric Oxide. John Wiley & Sons.
El-Bayaa, A.A., Badawy, N.A., AlKhalik, E.A., 2009. Effect of ionic strength on the adsorption of copper and chromium ions by vermiculite pure clay mineral. J. Hazard. Mater. 170, 1204–1209.
Goldberg, S., 2005. Inconsistency in the triple layer model description of ionic strength dependent boron adsorption. J. Colloid Interface Sci. 285, 509–517.
Gu, X., Evans, L.J., 2007. Modelling the adsorption of Cd(II), Cu(II), Ni(II), Pb(II), and Zn (II) onto Fithian illite. J. Colloid Interface Sci. 307, 317–325.
Gu, X., Evans, L.J., 2008. Surface complexation modelling of Cd(II), Cu(II), Ni(II), Pb(II) and Zn(II) adsorption onto kaolinite. Geochimica Cosmochimica Acta 72, 267–276.
Gu, X., Evans, L.J., Barabash, S.J., 2010. Modeling the adsorption of Cd (II), Cu (II), Ni (II), Pb (II) and Zn (II) onto montmorillonite. Geochimica Cosmochimica Acta 74, 5718–5728.
Gu, C., Wang, Z., Kubicki, J.D., Wang, X., Zhu, M., 2016. X-ray adsorption spectroscopic quantification and speciation modeling of sulfate adsorption on ferrihydrite surfaces. Environ. Sci. Technol. 50, 8067–8076.
Hao, W., Flynn, S.L., Alessi, D.S., Konhauser, K.O., 2018. Change of the point of zero net proton charge (pHPZNPC) of clay minerals with ionic strength. Chem. Geol. 493, 458–467.
Hao, W., Pudasainee, D., Gupta, R., Kashiwabara, T., Alessi, D.S., Konhauser, K.O., 2019. Effect of acidic conditions on surface properties and metal binding capacity of clay minerals. ACS Earth Space Chem Just accepted.
Hizal, J., Apak, R., 2006. Modeling of copper(II) and lead(II) adsorption on kaolinite-based clay minerals individually and in the presence of humic acid. J. Colloid Interface Sci. 295, 1–13.
Hohl, H., Stumm, W., 1976. Interaction of Pb2+ with hydrous γ-Al2O3. J. Colloid Interface Sci. 55, 281–288.
Ikhsan, J., Wells, J.D., Johnson, B.B., Angove, M.J., 2005. Surface complexation modeling of the sorption of Zn(II) by montmorillonite. Colloids and Surfaces A 252, 33–41.
Kallay, N., Kovačević, D., Žalac, S., 2006. Chapter 6 - thermodynamics of the solid/liquid interface - its application to adsorption and colloid stability. In: Johannes, L. (Ed.), Interface Science and Technology. Elsevier, pp. 133–170.
Kashiwabara, T., Takahashi, Y., Tanimizu, M., Usui, A., 2011. Molecular-scale mechanisms of distribution and isotopic fractionation of molybdenum between seawater and ferromanganese oxides. Geochimica Cosmochimica Acta 75, 5762–5784.
Kaya, A., Yukselen, Y., 2005. Zeta potential of clay minerals and quartz contaminated by heavy metals. Can. Geotech. J. 42, 1280–1289.
Kraepiel, A.M.L., Keller, K., Morel, F.M.M., 1998. On the acid-base chemistry of permanently charged minerals. Environ. Sci. Technol. 32, 2829–2838.
Lackovic, K., Angove, M.J., Wells, J.D., Johnson, B.B., 2003. Modeling the adsorption of Cd(II) onto Muloorina illite and related clay minerals. J. Colloid Interface Sci. 257, 31–40.
Lalonde, S.V., Amskold, L.A., Warren, L.A., Konhauser, K.O., 2007. Surface chemical reactivity and metal adsorptive properties of natural cyanobacterial mats from an alkaline hydrothermal spring, Yellostone National Park. Chem. Geol. 243, 36–52.
Landry, C.J., Koretsky, C.M., Lund, T.J., Schaller, M., Das, S., 2009. Surface complexation modeling of Co(II) adsorption on mixtures of hydrous ferric oxide, quartz and kaolinite. Geochimica Cosmochimica Acta 73, 3723–3737.
Langmuir, D., 1997. Aqueous Environmental Geochemistry. Prentice-Hall, Inc.
Liu, Y., Alessi, D.S., Flynn, S.L., Alam, M.S., Hao, W., Gingras, M., Zhao, H., Konhauser, K.O., 2018. Acid-base properties of kaolinite, montmorillonite and illite at marine ionic strength. Chem. Geol. 483, 191–200.
Lyons, T.W., Anbar, A.D., Severmann, S., Scott, C., Gill, B.C., 2009. Tracking euxinia in the ancient ocean: a multiproxy perspective and Proterozoic case study. Annu. Rev. Earth Planet. Sci. 37, 507–534.
McBride, M., 1989. Reactions Controlling Heavy Metal Solubility in Soils, Advances in Soil Science. Springer, pp. 1–56.
Morton, J.D., Semrau, J.D., Hayes, K.F., 2001. An X-ray absorption spectroscopy study of

the structure and reversibility of copper adsorbed to montmorillonite clay. Geochimica Cosmochimica Acta 65, 2709–2722.
Partin, C.A., Bekker, A., Planavsky, N.J., Scott, C.T., Gill, B.C., Li, C., Podkovyrov, V., Maslov, A., Konhauser, K.O., Lalonde, S.V., Love, G.D., Poulton, S.W., Lyons, T.W., 2013. Large-scale fluctuations in Precambrian atmospheric and oceanic oxygen levels from the record of U in shales. Earth Planet. Sci. Lett. 369–370, 284–293.
Peacock, C.L., Sherman, D.M., 2005. Surface complexation model for multisite adsorption of copper(II) onto kaolinite. Geochimica Cosmochimica Acta 69, 3733–3745.
Reich, T.J., Das, S., Koretsky, C.M., Lund, T.J., Landry, C.J., 2010. Surface complexation modeling of Pb(II) adsorption on mixtures of hydrous ferric oxide, quartz and kaolinite. Chem. Geol. 275, 262–271.
Reinhard, C.T., Planavsky, N.J., Robbins, L.J., Partin, C.A., Gill, B.C., Lalonde, S.V., Bekker, A., Konhauser, K.O., Lyons, T.W., 2013. Proterozoic Ocean redox and biogeochemical stasis. Proc. Natl. Acad. Sci. 110, 5357–5362.
Reinhard, C.T., Planavsky, N.J., Gill, B.C., Ozaki, K., Robbins, L.J., Lyons, T.W., Fischer, W.W., Wang, C.J., Cole, D.B., Konhauser, K.O., 2017. Evolution of the global phosphorus cycle. Nature 541, 386–389.
Sahai, N., Sverjensky, D.A., 1997. Solvation and electrostatic model for specific electrolyte adsorption. Geochimica Cosmochimica Acta 61, 2827–2848.
Schaller, M.S., Koretsky, C.M., Lund, T.J., Landry, C.J., 2009. Surface complexation modeling of Cd(II) adsorption on mixtures of hydrous ferric oxide, quartz and kaolinite. J. Colloid Interface Sci. 339, 302–309.
Schroth, B.K., Sposito, G., 1998. Effect of landfill leachate organic acids on trace metal adsorption by kaolinite. Environ. Sci. Technol. 32, 1404–1408.
Scott, C., Lyons, T., Bekker, A., Shen, Y., Poulton, S., Chu, X., Anbar, A., 2008. Tracing the stepwise oxygenation of the Proterozoic Ocean. Nature 452, 456.
Scott, C., Planavsky, N.J., Dupont, C.L., Kendall, B., Gill, B.C., Robbins, L.J., Husband, K.F., Arnold, G.L., Wing, B.A., Poulton, S.W., 2013. Bioavailability of zinc in marine systems through time. Nat. Geosci. 6, 125–128.
Sinitsyn, V.A., Aja, S.U., Kulik, D.A., Wood, S.A., 2000. Acid-base surface chemistry and sorption of some lanthanides on K^+-saturated marblehead illite: I. results of an experimental investigation. Geochimica Cosmochimica Acta 64, 185–194.
Sposito, G., Skipper, N.T., Sutton, R., Park, S., Soper, A.K., Greathouse, J.A., 1999. Surface geochemistry of the clay minerals. Proc. Natl. Acad. Sci. 96, 3358–3364.
Sverjensky, D.A., Sahai, N., 1996. Theoretical prediction of single-site surface-protonation equilibrium constants for oxides and silicates in water. Geochimica Cosmochimica Acta 60, 3773–3797.
Tertre, E., Castet, S., Berger, G., Loubet, M., Giffaut, E., 2006. Surface chemistry of kaolinite and Na-montmorillonite in aqueous electrolyte solutions at 25 and 60°C: Experimental and modeling study. Geochimica Cosmochimica Acta 70, 4579–4599.
Tribovillard, N., Algeo, T.J., Lyons, T., Riboulleau, A., 2006. Trace metals as paleoredox and paleoproductivity proxies: an update. Chem. Geol. 232, 12–32.
Vane, L.M., Zang, G.M., 1997. Effect of aqueous phase properties on clay particle zeta potential and electro-osmotic permeability: implications for electro-kinetic soil remediation processes. J. Hazard. Mater. 55, 1–22.
Veselska, V., Fajgar, R., Cihalova, S., Bolanz, R., Gottlicher, J., Steininger, R., Siddique, J., Komarek, M., 2016. Chromate adsorption on selected soil minerals: surface complexation modeling coupled with spectroscopic investigation. J. Hazard. Mater. 318, 433–442.
Wang, X., Wang, Z., Peak, D., Tang, Y., Feng, X., Zhu, M., 2018. Quantification of coexisting inner- and outer-sphere complexation of sulfate on hematite surfaces. ACS Earth and Space Chemistry 2, 387–398.
Westall, J.C., 1982. FITEQL: A Computer Program for Determination of Chemical Equilibrium Constants Form Experimental Data. Department of Chemistry. Oregon State University.
Wu, X.L., Zhao, D., Yang, S.T., 2011. Impact of solution chemistry conditions on the sorption behavior of Cu(II) on Lin'an montmorillonite. Desalination 269, 84–91.
Xu, D., Zhou, X., Wang, X., 2008. Adsorption and desorption of Ni2+ on Na-montmorillonite: effect of pH, ionic strength, fulvic acid, humic acid and addition sequences. Appl. Clay Sci. 39, 133–141.
Xu, R., Wang, Y., Tiwari, D., Wang, H., 2009. Effect of ionic strength on adsorption of As (III) and As(V) on variable charge soils. J. Environ. Sci. 21, 927–932.